Meteorologische Zeitschrift, Vol. **19**, No. 6, 539-547 (December 2010)

Article

A numerical case study on footprint model performance under inhomogeneous flow conditions

TIINA MARKKANEN[1,4], GERALD STEINFELD[2,5], NATASCHA KLJUN[3], SIEGFRIED RAASCH[2] and THOMAS FOKEN[1*]

[1]Department of Micrometeorology, University of Bayreuth, Bayreuth, Germany
[2]Institute of Meteorology and Climatology, Leibniz University of Hanover, Hanover, Germany
[3]Department of Geography, School of the Environment and Society, Swansea University, Swansea, UK
[4]now: Climate and Global Change Research, Finnish Meteorological Institute, Helsinki, Finland
[5]now: ForWind – Center for Wind Energy Research, Institute of Physics, Carl-von-Ossietzky-University of Oldenburg, Oldenburg, Germany

(Manuscript received April 27, 2009; in revised form February 12, 2010, accepted August 4, 2010)

Abstract

Two models for predicting near-surface flux and concentration footprints are compared concerning their performance in the presence of heterogeneous surface conditions. One of the models is a conventional Lagrangian backward model and the second an LES model with an embedded Lagrangian footprint model. The latter model reveals generation of thermally induced secondary circulation under such surface heterogeneity. The conventional Lagrangian backward model with simple parameterization of flow conditions mostly performs well in footprint predictions for concentrations and somewhat worse for fluxes, and fails only in areas where flow patterns are dominated by pronounced secondary circulations.

Zusammenfassung

Zwei Modelle zur Bestimmung der bodennahen Fluss- und Konzentrationsfootprints werden hinsichtlich ihrer Leistungsfähigkeit für heterogene Unterlagenbedingungen verglichen. Das erste Modell war ein konventionelles Lagrangesches Rückwärtsmodell und das zweite ein LES Modell mit eingebetteter Lagrangescher Footprintmodellierung. Letzteres zeigt die Entstehung von thermisch induzierten Sekundärzirkulationen unter heterogenen Bedingungen. Das konventionelle Lagrangesche Rückwärtsmodell erfüllte weitgehend die Footprintbestimmung selbst mit einer einfachen Parametrisierung der Strömungsbedingungen. Es versagt lediglich in den Gebieten, die von den Sekundärzirkulationen dominiert wurden.

1 Introduction

Concentrations and fluxes at a given point in the atmospheric boundary layer are influenced from a surface area on the windward side of the measuring point. Each point within this area has a different influence on the measuring signal. Footprint modelling aims at determining the areas of greatest influence on concentrations or fluxes of atmospheric constituents at a certain location. The impact of the fluxes of the source area on the measured signal is described by the footprint function. Determination of the footprint is necessary for interpretation of the results of measurements, especially when these are performed over a landscape of varying surface source strengths. Varying source strength is often related to patchiness of the properties of the underlying surface, which in turn is often reflected as heterogeneity of the flow field. Contradicting these facts, however, horizontal homogeneity is a fundamental requirement of most of the existing footprint models (FOKEN and LECLERC, 2004).

For 20 years a mathematical description of footprint function replaced more empirical assumptions based on a proposal by GASH (1986). Recently, several overview papers were published (SCHMID, 2002, VESALA et al., 2008, VESALA et al., 2004). The most common footprint models are listed in FOKEN (2008). Analytical footprint models are similar to the air pollution modelling with an analytic solution for the diffusion equation and are usually applied only in the atmospheric surface layer (ASL) where Monin-Obukhov scaling is valid.

In the stochastic Lagrangian (LS) approach, in turn, a large number of particles is transported either backward (e.g. KLJUN et al., 2002) or forward (e.g. LECLERC and THURTELL, 1990, RANNIK et al., 2000) in time. The calculation of these models is more time consuming but they can also be applied for measurements over tall vegetation. In particular, forward LS models require very large particle numbers for resolving local footprints under heterogeneous flow conditions. Thus they are usually used for homogeneous flow fields where the inverted plume assumption can be applied.

The backward approach is more suitable for horizontally heterogeneous flow conditions, as the particles are released from unambiguous measurement positions and

*Corresponding author: Thomas Foken, Department of Micrometeorology, University of Bayreuth, Universitätsstrasse 30, 95440 Bayreuth, Germany, e-mail: thomas.foken@uni-bayreuth.de

DOI 10.1127/0941-2948/2010/0488

0941-2948/2010/0488 $ 4.05

Table 1: Driving parameters for LPDM-B and averages of the respective flow characteristics of sub-domains as derived from LES results. Symbols in the table are as follows: friction velocity ($u*$), Obukhov length (L), convective velocity scale ($w*$) and boundary layer height (z_i).

Main split of the domain	Warm area 1920 m x 3840 m (West)	Cooler area 1920 m x 3840 m (East)
Kinematic heat flux (Km s^{-1})	0.15	0.05
$u*$ (ms^{-1})	0.23	0.16
$w*$ (ms^{-1})	1.745	0.944
z_i (m)	1094.8	527.1
L (m)	–5.59	–6.11
Further split of subdomain acc. to flow characteristics	Nearest 460 m x 3840 m, West from dividing line	Nearest 460 m x 3840 m East from dividing line
$u*$ (ms^{-1})	0.237	0.177
$w*$ (ms^{-1})	1.329	0.913
z_i (m)	492.1	474.0
L (m)	6.28	7.47

followed towards their sources. However, similar to forward LS models, it suffers from the lack of a simple description of the heterogeneous flow fields. This problem can be overcome by pre-determining a detailed flow field with large eddy simulation (LES) which is subsequently used for Lagrangian footprint determination. This approach was used by CAI and LECLERC (2007) in both backward and forward simulations. STEINFELD et al. (2008) developed an LES approach in which both turbulence statistics and turbulent dispersion of particles are calculated simultaneously. Even though this is effectively a forward approach, the method facilitates calculations for a large number of particles. In this work we determine footprints at various heights over a surface with well defined heterogeneity in surface conditions. As the heterogeneity is given as a step change of surface properties in the surroundings of the measurement point, in the LES case this will lead to a flow pattern consisting of the component of the background wind direction and a component due to a secondary circulation driven by the heterogeneity. Thus, the local wind properties at an arbitrary observation point vary according to the distance from the heterogeneity and observation height.

For the case study on surface heat flux heterogeneity presented in this work we use the LES model PALM (RAASCH and SCHRÖTER, 2001) that has been coupled with a Lagrangian stochastic forward model for the evaluation of particle trajectories (STEINFELD et al., 2008). Because LES requires so much CPU time, it cannot be used as a routine tool for estimating footprints of measurements. Thus, we assess the performance of a Lagrangian stochastic backward footprint model (LPDM-B, KLJUN et al., 2002) using simple parameterizations accounting for the heterogeneity. The performance of these two models together with a LS forward model by RANNIK et al. (2000) under horizontally homogeneous flow conditions was studied by MARKKANEN et al. (2009).

2 Models

2.1 LES-model PALM

The LS particles are embedded into the LES model PALM (RAASCH and SCHRÖTER, 2001) which covers a wide range of boundary layer stratifications. The method for particle inclusion is based on WEIL et al. (2004) where the particle velocities are separated into two parts, following the fundamental LES idea of dividing the turbulent flow field into an explicitly resolved grid scale part and a modelled sub-grid scale part. For stochastic transport WEIL et al. (2004) adapted the THOMSON (1987) model which assumes isotropy and Gaussianity of turbulence (see WEIL et al. 2004, for more details). The grid scale flow characteristics are interpolated linearly in vertical, and bilinearly in horizontal, to sub-grid scale particle positions. Following KIM et al. (2005), no explicit boundary condition has been used at the boundary layer top.

Importantly, in the PALM embedded LS model we use, the particles are simulated online during the LES run. That is not the case in LES driven LS simulations by WEIL et al. (2004), CAI et al. (2006) and KIM et al. (2005) who use pre-calculated LES data for separate LS simulations. The latter method is costly in terms of the disc space required, and limited by writing and reading rates of the data. Furthermore, the LES embedded LS calculations are fully parallelised which facilitates release of an exceptionally high number of particles.

A horizontal domain decomposition as used in PALM (RAASCH and SCHRÖTER, 2001) is of especially great benefit in particle dispersal simulations; this is because vertically the particles remain in the lower part of the domain, whereas horizontally they simultaneously cover a relatively large fraction of the domain. In fact, the particles are not expected to reach the uppermost heights of the domain at all as they are strongly bounced back at the top of the boundary layer. Thus, vertical domain

decomposition would not be as effective as the horizontal decomposition as the boundary layer parts would require much more computing time than those above. For a more detailed description of the approach see STEINFELD et al. (2008).

The footprint contributions for fluxes and concentrations can be derived according to the KURBANMURADOV et al. (2001) approach for forward dispersal data. A detailed description of the application of the approach in the context of PALM LES model is given in STEINFELD et al. (2008) and MARKKANEN et al. (2009) for horizontally homogeneous flow conditions. However, in the case of horizontally heterogeneous flow, instead of using all the particles crossing the measurement level (see MARKKANEN et al., 2009), only the particles travelling through a horizontal stripe of a given width, parallel to the heterogeneity, can be considered. In effect, this means that instead of providing point measurements, a sensor has a horizontal dimension equal to the width of the stripe where particles were counted, referred to in the following as the effective sensor sizes (STEINFELD et al., 2008). In the LES approach of this study the restricted area for counting particle crossings was compensated by very large number of simulated particles. The LES embedded footprint approach was used in this paper as a reference because the description of physics by LES is more realistic and it was extensively compared against other LES results by STEINFELD et al. (2008) and against conventional LS models by MARKKANEN et al. (2009).

2.1.1 Backward model LPDM-B

In the present study, we use the backward Lagrangian footprint model LPDM-B. The model's dispersion module satisfies the well mixed condition by THOMSON (1987) from convective to stable stratifications and over the whole depth of the atmospheric boundary layer. We use the model in its most parameterized form in which only surface roughness length (z_0), friction velocity ($u*$), Obukhov length (L), convective velocity scale ($w*$) and boundary layer height (z_i) are required as inputs. Parameterizations of the mean wind speed profiles and standard deviations are described in ROTACH et al. (1996) and have been tested for many boundary layer conditions (cf. KLJUN et al., 2004). Calculation of backward trajectories and the method of deriving the flux and concentration footprints from the release and touchdown velocity data are described in FLESCH et al. (1995) and FLESCH (1996). For a detailed description and sensitivity analysis of LPDM-B the reader is referred to KLJUN et al. (2002).

In this work, in order to consider the heterogeneity of surface properties, the dispersion domain is parameterized with two separate sets of the above listed input parameters of LPDM-B. Corresponding flow field characteristics extend vertically throughout the entire boundary layer and are not bent downwind as a more realistic model for internal boundary layer development upwind from surface heterogeneity would require. Furthermore, in the present simple adaptation of the surface heterogeneity in the backward footprint model, wind direction is preserved even in the crossing of the heterogeneity, which is an obvious violation of conservation laws. Wind direction does not change in the vertical either.

3 Simulations

In this work PALM is driven in its dry mode and cyclic lateral boundaries are applied. Furthermore, Monin-Obukhov similarity is applied between the surface and the first computational grid point level. Coriolis force is not considered in these simulations. Aerodynamic roughness length was set to 0.16 m. The horizontal and vertical resolutions were 10 m. The domain, with total size 3840 m x 3840 m, was split into two equally wide parts that were driven by different surface heat fluxes (Table 1) after a spin-up time of 7200 s with a heat flux of 0.1 K m s^{-1}. The mean wind direction in the free atmosphere was set parallel to the line dividing the two areas and the mean wind velocity was 2 m s^{-1}. For more details see STEINFELD et al. (2008). After 4 h of simulation time, altogether 14,745,600 particles were released within a half hour period. As the effective sensor sizes were 20 m, 40 m and 80 m, the effective numbers used for footprint determination were 76,800, 153,600 and 307,200 respectively.

The two parameter sets derived from LES data (Table 1) were subsequently used in LBDM-B for parameterisation of the flow at both sides of the border dividing the two areas with different near-surface heat flux in the LES model domain. The particle number used for LBDM-B was around 180,000 in each simulation.

In the following discussion, the y-axis (South-North) is set parallel to the mean wind in the free atmosphere, thus the flow field is invariant along the y-axis. We calculated the footprints for several positions in the vicinity of the location of surface heat flux change and for positions in the middle of each half, i.e. at x = –960 m, –100 m, –50 m –10 m, 0 m, 10 m, 50 m, 100 m and 960 m. In backward model simulations the parameters for the locations within a distance of 460 m from the dividing line are given in the lower part of the Table 1, whereas the general parameters for the whole domain were used for the positions x = 960 m (Table 1 upper part). The LES footprints were derived for heights z = 3 m, 5 m, 10 m, 20 m, 30 m, 50 m, 100 m, 200 m and 500 m. A measurement height of z_m = 30 m was selected as the basic level for comparison between LES and backward models. In order to visualise the model predictions we estimate the smallest areas contributing 50 % and 80 % to the concentration and flux signals. According to SCHMID and OKE (1990), MARKKANEN et al. (2009) denoted these areas as Ω_P where P stands for the respective percentage of the total concentration or flux originating from

Table 2: Percentage contributions to the total concentration signals predicted by both models from overlapping footprint areas of given percentage levels. Values calculated for grid resolutions of 40 m. PALM stands for the LES model used in the study and LPDM-B refers to the backward LS model.

Measurement position	Signal from $\Omega^{\cap}{}_{50}$ (%)		Signal from $\Omega^{\cap}{}_{80}$ (%)	
	PALM	LPDM-B	PALM	LPDM-B
50 m West	36.0	35.6	53.5	56.9
10 m East	38.9	32.5	53.5	56.4
960 m West	15.9	27.5	30.9	51.5
960 m East	28.9	28.6	57.5	59.6

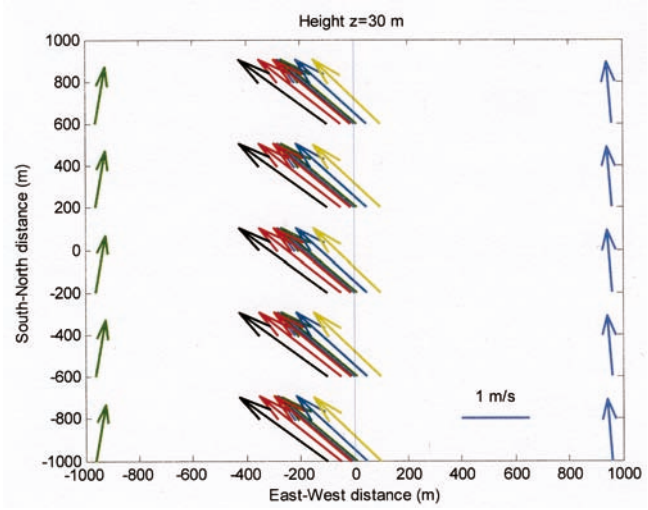

Figure 1: Wind vectors at measurement positions 960 m, 100 m, 50 m, 10 m and 0 m west and 10 m, 50 m, 100 m and 960 m east of the dividing line (colours green to blue respectively) at an observation height of 30 m. The warm surface is to the west and the cooler surface to the east from the border between the two areas indicated with a blue line. The velocity field has been obtained by temporal averaging over the period between 4 h and 5 h after the start of the LES simulation and by subsequent spatial averaging along the y-direction. Note that, therefore, the velocity field does not vary along the y-direction, but only along the x-direction.

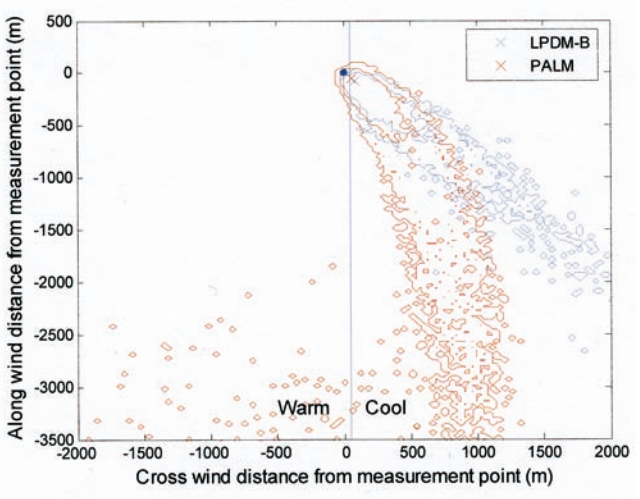

Figure 2: Concentration footprints from the conventional backward LS model LPDM-B (blue contour) and LES model PALM (red contour) at z_m = 30 m. Measurement position is at (0,0) and the step change of surface properties (blue line) is 50 m east of the measurement position. Contours indicate the smallest areas contributing 50 % and 80 % of the total concentration signal (i.e. contribution from the whole domain area). The crosses indicate the respective location of the maximum of the footprint function and the dot indicates the measurement point. Grid resolution is 30 m.

the domain. For quantitative assessment of the agreement between the models the signals originating from overlapping Ω_P's are given (i.e signals from areas $\Omega^{\cap}{}_P$ as denoted in MARKKANEN et al., 2009).

4 Results

4.1 Flow fields

The wind field at the height of z_m = 30 m (Figure 1) resembles those of other observation heights up to z_m = 200 m. Close to the dividing line of surface properties south-easterlies are prevailing, while in the middle of each half (x = 960 m) the winds are nearly southerlies.

At z_m = 500 m all the wind directions are close to the free atmosphere mean wind direction (see Figure 11 in STEINFELD et al., 2008), while at yet higher levels the wind pattern turns to a mirror image of that of at 30 m. In other words, negative values of the u-component at heights z < 500 m turn positive at heights z > 500 m and vice versa. This finding indicates the existence of secondary circulations in the atmospheric boundary layer as reported previously by e.g. PATTON et al. (2005), LETZEL and RAASCH (2003) and AVISSAR and SCHMIDT (1998). As the surface roughness is constant within the domain, the secondary circulation is solely due to heterogeneity in the heat flux of the surface. The averaging period for this analysis was 2 hours.

4.2 Concentration footprints

In the following discussion the measurement position is set to origin; the y-axis is parallel to the mean wind in the free atmosphere with values growing from south to north, while the x-axis is the west-east axis. LES derived concentration footprints for measurement positions 50 m west and 10 m east of the dividing line are

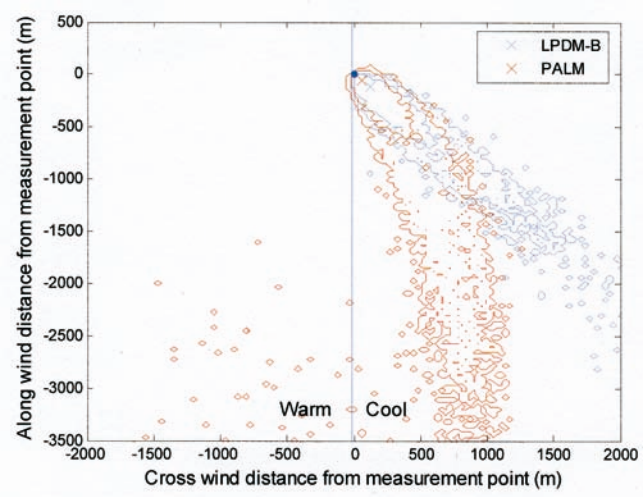

Figure 3: Concentration footprints from the conventional backward LS model LPDM-B (blue contour) and the LES model PALM (red contour) at $z_m = 30$ m. Measurement position is at (0,0) and the step change of surface properties (blue line) is 10 m west of the measurement position. See the figure caption of Figure 2 for explanation of contours and crosses.

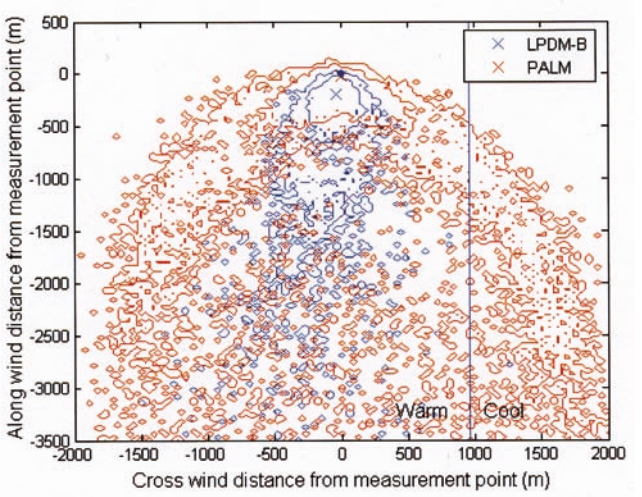

Figure 4: Concentration footprints from the conventional backward LS model LPDM-B (blue contour) and LES model PALM (red contour) at $z_m = 30$ m. Measurement position is at (0,0) and the step change of surface properties (blue line) is 960 m east of the measurement position. See the figure caption of Figure 2 for explanation of contours and crosses.

very similar to each other (Figure 2 and 3) and consequently also very similar to footprints for positions in between, including the one with measurement position directly above the change in surface properties (not shown). The most prominent footprint areas close to the peak position as predicted by the two models show high agreement both in location and width. The main difference between the two models is found in the tails of the footprints. While that of the backward model extends directly upwind according to the south-westerly wind direction at the measurement point, the LES predicted footprint turns towards the south. The latter behaviour is due to the thermally induced secondary circulation with southerly wind direction at distances corresponding to the location of the tail (Figure 1) and at higher levels of the boundary layer. This pattern cannot be considered by the backward model which was only provided with the mean wind direction at the measurement position. At a distance of 100 m west of the dividing line the LES model derived footprint is somewhat narrower than in the previous two cases (not shown), whereas at the same distance east of the dividing line (not shown) the LES model derived footprint is very similar to those closer to the line (Figures 2 and 3). This is a consequence of the modified flow field due to the thermal secondary circulation leading to acceleration of air towards the centre of the warmer area.

With a measurement location at a distance of 960 m west of the dividing line the concentration footprints predicted by both models differ most, also close to the measurement positions (Figure 4). This was the most pronounced disagreement observed in this study. While the footprint predicted by the backward model is slightly wider compared to that over the cooler half of the do-

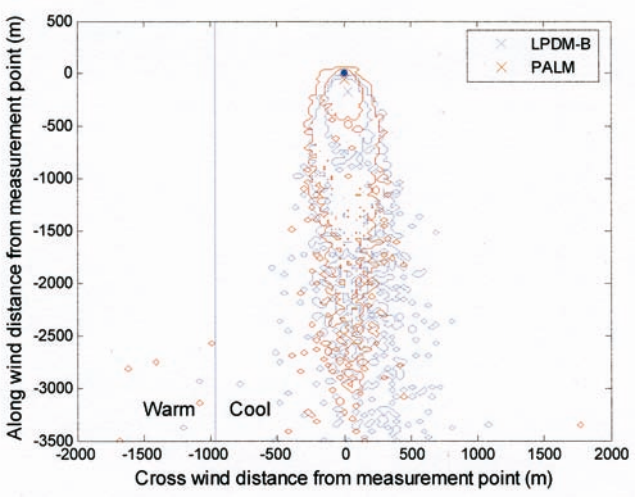

Figure 5: Concentration footprints from the conventional backward LS model LPDM-B (blue contour) and LES model PALM (red contour) at $z_m = 30$ m. Measurement position is at (0,0) and the step change of surface properties (blue line) is 960 m west of the measurement position. See the figure caption of the Figure 2 for explanation of contours and crosses.

main (Figure 5), the footprint from LES model shows two prominent branches with tails extending first south-east and south-west and eventually bending towards the south. The two branch pattern of LES is due to convergence of horizontal wind at the measurement position where the most prominent convective updraft is located (see Figure 1 and STEINFELD et al., 2008, Figure 11 for the wind field throughout the boundary layer). This pattern cannot be predicted by the parameterisation used for the backward LS model in which case the influence of surface heat flux is rather of a local nature.

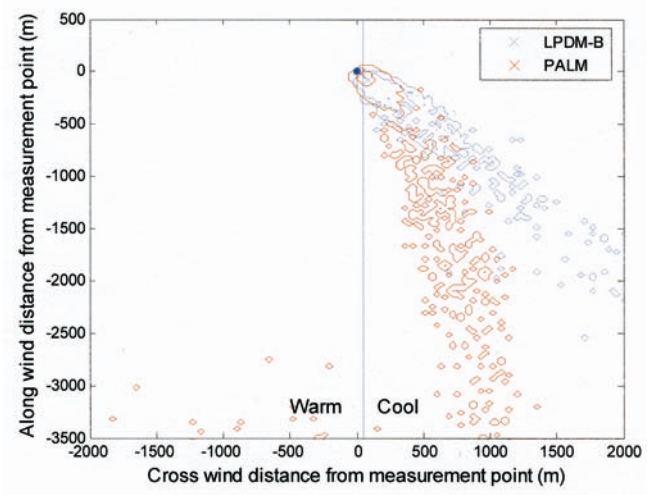

Figure 6: . Flux footprints from the conventional backward LS model LPDM-B (blue contour) and LES model PALM (red contour) at $z_m = 30$ m. Measurement position is at (0,0) and the step change of surface properties (blue line) is 50 m east of the measurement position. Contours indicate the smallest areas contributing 80 % and 50 % of the total positive flux signal (i.e. sum of positive contribution from the whole domain area. The areas of negative flux footprint due to secondary circulation are neglected). The crosses indicate the respective location of the maximum of the footprint function and the dot indicates the measurement point. Grid resolution is 30 m.

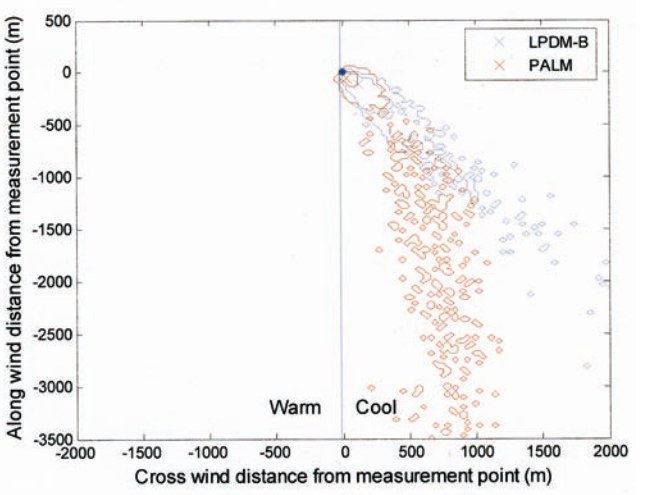

Figure 7: Flux footprints from the conventional backward LS model LPDM-B (blue contour) and LES model PALM (red contour) at $z_m = 30$ m. Measurement position is at (0,0) and the step change of surface properties (blue line) is 10 m west of the measurement position. See the figure caption of the Figure 6 for explanation of contours and crosses.

At a distance of 960 m east of the dividing line the concentration footprints are slightly wider in the cross-wind direction than those closer to the dividing line (Figure 5). Even though the backward model LPDM-B predicts a peak position somewhat more upwind than the LES model PALM does, agreement between the predictions of both models is very good.

Quantitative comparison of the concentration signals originating from $\Omega^{\cap}{}_{50}$ and $\Omega^{\cap}{}_{80}$ confirms the visual inspection (Table 2). These results do support the conclusions drawn based on the visual inspection, the location over the cooler half of the domain (960 m east from the border) producing highest agreement between the models among the four locations studied. However, because the data is very scattered due to relatively low effective particle numbers, these results are very sensitive to grid size.

4.3 Flux footprints

While PALM predicts, for 80 % of the signal, larger concentration footprint areas than LPDM-B does, the flux footprints for the observation positions in the middle of the domain show opposite behavior. For an observation point 50 m west of the dividing line (Figure 6) the flux footprint predictions from both models are of approximately the same width. However, the LES derived footprint has its maximum very close to the measurement position and its most prominent part decreases within 200 m from the maximum. This is due to the secondary circulation bringing descending particles to the area, which cancel out the positive contribution of ascending particles to the flux. The tail of the flux footprint, even though it makes a relatively low contribution to the flux, is positioned similarly to that of the corresponding concentration footprint (Figure 2). As a simple parameterization for wind direction is used in LPDM-B, the footprint aligns with the mean wind at the measurement point. The results for an observation point 10 m east of the dividing line show similar behaviour (Figure 7).

At the position 960 m west of the dividing line, the flux footprints (Figure 8) show close resemblance to the respective concentration footprints (Figure 4). The LES predicted footprint consists of a wide central part with two tails bending south at both sides. Pronounced fading off by descending particles is not observed here, which is due to positive mean vertical winds over the warm surface.

At a measurement position 960 m east of the dividing line (Figure 9) the fading off of the tail of the LES predicted footprint is more pronounced than in Figure 6 and 7. Otherwise the footprints predicted by both models are very symmetrical across the mean wind direction and of approximately the same widths.

Comparison of flux signals from the overlapping footprint areas (Table 3) shows, overall, worse agreement than that of concentrations. The result supports the qualitative visual judgment that the most prominent LES footprint is largely enclosed by the one predicted by LBDM-B, with the exception of the measurement position 960 m west from the dividing line.

Table 3: Percentage contributions to the total concentration signals predicted by both models from overlapping footprint areas of given percentage levels. Values calculated for grid resolutions of 40 m. PALM stands for the LES model used in the study and LPDM-B refers to the backward LS model.

Measurement position	Signal from $\Omega^{\cap}{}_{50}$ (%)		Signal from $\Omega^{\cap}{}_{80}$ (%)	
	PALM	LPDM-B	PALM	LPDM-B
50 m West	11.8	1.4	61.6	14.1
10 m East	32.6	2.3	78.8	11.3
960 m West	5.7	6.0	31.3	65.2
960 m East	7.2	2.3	29.5	34.4

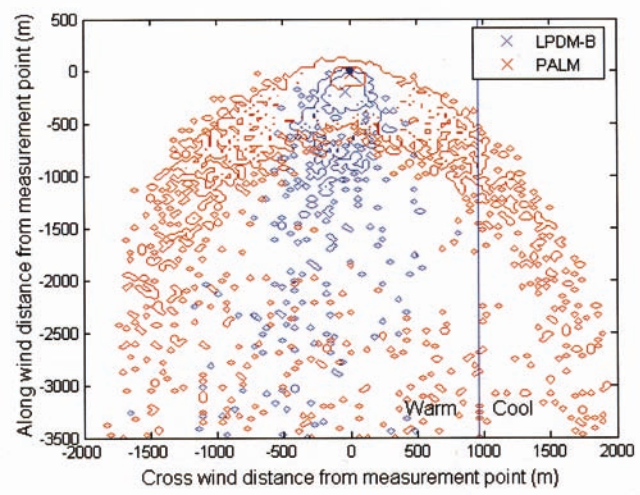

Figure 8: Flux footprints from the conventional backward LS model LPDM-B (blue contour) and LES model PALM (red contour) at $z_m = 30$ m. Measurement position is at (0, 0) and the step change of surface properties (blue line) is 960 m east of the measurement position. See the figure caption of the Figure 6 for explanation of contours and crosses.

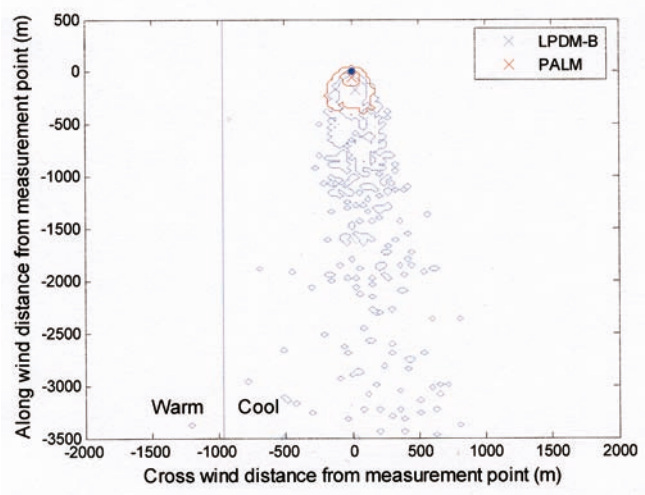

Figure 9: Flux footprints from the conventional backward LS model LPDM-B (blue contour) and LES model PALM (red contour) at $z_m = 30$ m. Measurement position is at (0,0) and the step change of surface properties (blue line) is 960 m west of the measurement position. See the figure caption of the Figure 6 for explanation of contours and crosses.

Finally, in order to make sure that the two tail pattern of the footprints is not an artefact due to large sensor size we made test runs with the sensor size reduced down to 1 m. As even these results (not shown), in spite of being of reduced statistical reliability, predicted the two tail structure of a footprint at the measurement point over the warm part of the domain, we can conclude that the larger sensor sizes give a realistic footprint pattern (see also STEINFELD et al., 2008).

5 Conclusions

This work aimed at studying the applicability of a conventional backward LS model with a highly simplified parameterization of heterogeneity under flow conditions characterized by a secondary circulation. The flux and concentration footprints predicted by the two models used in the study – the LES model PALM embedded particle dispersion model and backward LS model LPDM-B – seemed to agree well for the most prominent parts of the footprint areas. Around the peak position which indicates the location of the highest importance to the signals, the two footprint predictions were generally of similar width and shape. In all studied cases the LES model predicted peak positions closer to the measurement point than the backward LS model LPDM-B. The concentration footprints, in particular, showed high agreement except for the tails of the areas accounting for 80 % of the total signals from within the domain of 3840 m x 3840 m, and the agreement of the signals originating from overlapping footprint areas of certain percentage (Ω_P) also supported this judgement. The influence of secondary circulation is of higher importance in the case of flux footprints as descending particles reduce the contribution of their rising companions at some areas of the domain in the LES predictions. PATTON et al. (2005) concluded that a single point measurement in this heterogeneous setup would not equate to areal averaged flux. Using the same LES model PALM as applied here, INAGAKI et al. (2006) found that neglecting the mesoscale flux can result in an underestimation of several tens of percent of the areal averaged flux. However, imbalance statistics were not calculated for the simulation presented in this paper.

The parameterization used for LPDM-B to account for the step change in surface properties assumed local balance of the flow field with underlying surface throughout the boundary layer. This approach does not consider development of balance downwind from the step change (in other words the structure of internal boundary layer), moreover the approach is by no means able to produce the wind field predicted by LES that is related to the thermal secondary circulation generated under the heterogeneous pattern of near surface heat flux used in this study. Consequently the backward LS model with this parameterization fails to produce the two tail pattern of footprints in the middle of the warm surface where the horizontal wind field converges according to LES close to the surface. However, usually footprint models are applied to measurements performed in towers at fixed positions and consequently the data available for model calibration is local by nature.

All in all, we conclude that the conventional backward LS model mostly performs well in footprint predictions even with a simple parameterization of flow conditions except for the most devious flow patterns with pronounced secondary circulations and a local horizontal convergence of the flow. PATTON et al. (2005) concluded that the relation of the length scale of the heterogeneity versus the boundary layer height determines the strength of the induced mesoscale flows. On the other hand, AVISSAR and SCHMIDT (1998) found that a mean velocity larger than 2.5 m s^{-1} is high enough to reduce the impact of land-surface heterogeneity. Thus, an extensive set of LES runs under different length scales of the heterogeneity would be useful in order to estimate the applicability of conventional footprint models under various heterogeneous conditions. Furthermore, more data from tracer experiments would be required to assess the LES results under heterogeneous conditions.

Acknowledgments

The project was funded by the German Science Foundation under the contracts FO 226/10-1, 2 and RA 617/16-1, 2, and by ETH, Zürich.

References

AVISSAR, R., T. SCHMIDT, 1998: An evaluation of the scale at which ground-surface heat flux patchiness affects the convective boundary layer using large-eddy simulation. – J. Atmos. Sci. **55**, 2666–2689.

CAI, X.H., M.Y. LECLERC, 2007: Forward-in-time and backward-in-time dispersion in the convective boundary layer: The concentration footprint. – Bound.-Layer Meteor. **123**, 201–218.

CAI, X.H., R. ZHANG, Y. LI, 2006: A large-eddy simulation and Lagrangian stochastic study of heavy particle dispersion in the convective boundary layer. – Bound-Layer Meteor. **120**, 413–435.

FLESCH, T.K., 1996: The footprint for flux measurements, from backward Lagrangian stochastic models. – Bound-Layer Meteor. **78**, 399–404.

FLESCH, T.K., J.D. WILSON, E. YEE, 1995: Backward-time Lagrangian stochastic dispersion models and their application to estimate gaseous emissions. – J. Appl. Meteor. **34**, 1320–1332.

FOKEN, T., 2008: Micrometeorology. – Springer, Berlin, Heidelberg, 308 pp.

FOKEN, T., M.Y. LECLERC, 2004: Methods and limitations in validation of footprint models. – Agric. Forest. Meteor. **127**, 223–234.

GASH, J.H.C., 1986: A note on estimating the effect of a limited fetch on micrometeorological evaporation measurements. – Bound.-Layer Meteor. **35**, 409–414.

INAGAKI, A., M.O. LETZEL, S. RAASCH, M. KANDA, 2006: Impact of surface heterogeneity on energy balance: A study using LES. – J. Meteor. Soc. Japan **84**, 187–198.

KIM, S.W., C.H. MOENG, J.C. WEIL, M.C. BARTH, 2005: Lagrangian particle dispersion modeling of the fumigation process using large-eddy simulation. – J. Atmos. Sci. **62**, 1932–1946.

KLJUN, N., M.W. ROTACH, H.P. SCHMID, 2002: A three-dimensional backward Lagrangian footprint model for a wide range of boundary layer stratification. – Bound.-Layer Meteor. **103**, 205–226.

KLJUN, N., P. KASTNER-KLEIN, E. FEDEROVICH, M.W. ROTACH, 2004: Evaluation of Lagrangian footprint model using data from wind tunnel convective boundary layer. – Agric. Forest. Meteor. **127**, 189–201.

KURBANMURADOV, O., Ü. RANNIK, K.K. SABELFELD, T. VESALA, 2001: Evaluation of mean concentration and fluxes in turbulent flows by Lagrangian stochastic models. – Math. Comp. Simul. **54**, 459–476.

LECLERC, M.Y., G.W. THURTELL, 1990: Footprint prediction of scalar fluxes using a Markovian analysis. –Bound.-Layer Meteor. **52**, 247–258.

LETZEL, M.O., S. RAASCH, 2003: Large-eddy simulation of thermally induced oscillations in the convective boundary layer. – J. Atmos. Sci. **60**, 2328–2341.

MARKKANEN, T., G. STEINFELD, N. KLJUN, S. RAASCH, T. FOKEN, 2009: Comparison of conventional Lagrangian stochastic footprint models against LES driven footprint estimates. – Atmos. Chem. Phys. **9**, 5575–5586.

PATTON, E.G., P.P. SULLIVAN, C.-H. MOENG, 2005: The influence of idealized heterogeneity on wet and dry planetary boundary layers coupled to the land surface. – J. Atmos. Sci. **62**, 2078–2097.

RAASCH, S., M. SCHRÖTER, 2001: PALM - A large-eddy simulation model performing on massively parallel computers. – Meteorol. Z. **10**, 363–372.

RANNIK, Ü., M. AUBINET, O. KURBANMURADOV, K.K. SABELFELD, T. MARKKANEN, T. VESALA, 2000: Footprint analysis for measurements over heterogeneous forest. – Bound.-Layer Meteor. **97**, 137–166.

ROTACH, M.W., S.-E. GRYNING, C. TASSONE, 1996: A two-dimensional Lagrangian stochastic dispersion model for daytime conditions. – Quart. J. Roy. Meteor. Soc. **122**, 367–389.

SCHMID, H.P., 2002: Footprint modeling for vegetation atmosphere exchange studies: A review and perspective. – Agric. Forest. Meteor. **113**, 159–184.

SCHMID, H.P., T.R. OKE, 1990: A model to estimate the

source area contributing to turbulent exchange in the surface layer over patchy terrain. – Quart. J. Roy. Meteor. Soc. **116**, 965–988.

STEINFELD, G., S. RAASCH, T. MARKKANEN, 2008: Footprints in homogeneously and heterogeneously driven boundary layers derived from a Lagrangian Stochstic particle model embedded into large-eddy simulation. – Bound.-Layer Meteor. **129**, 225–248.

THOMSON, D.J., 1987: Criteria for the selection of stochastic models of particle trajectories in turbulent flows. – J. Fluid Mech. **189**, 529–556.

VESALA, T., N. KLJUN, U. RANNIK, J. RINNE, A. SOGACHEV, T. MARKKANEN, K. SABELFELD, T. FOKEN, M.Y. LECLERC, 2008: Flux and concentration footprint modelling: State of the art. – Environm. Pollution **152**, 653–666.

VESALA, T., U. RANNIK, M.Y. LECLERC, T. FOKEN, K.K. SABELFELD, 2004: Foreword: Flux and concentration footprints. – Agric. Forest. Meteor. **127**, 111–116.

WEIL, J.C., P.P. SULLIVAN, C.H. MOENG, 2004: The use of large-eddy simulations in Lagrangian particle dispersion models. – J. Atmos. Sci. **61**, 2877–2887.